



Article

Evaporation Affects the In Vitro Deposition of Nebulized Droplet in an Idealized Mouth-Throat Model

Xueying Xia 1 , Ting Ding 1 , Xiaole Chen 1,* , Feng Tao 2 , Baobin Sun 2 , Tong Lu 2 , Jianwei Wang 1 , Yu Huang 1 and Yin Xu 3

- School of Energy and Mechanical Engineering, Nanjing Normal University, Nanjing 210042, China
- ² Zhongda Hospital, Southeast University, Nanjing 210009, China
- School of Electrical, Energy and Power Engineering, Yangzhou University, Yangzhou 225127, China
- * Correspondence: xlc@njnu.edu.cn

Abstract: Nebulizer is one of inhalation therapy's most widely used aerosol generation devices. Nowadays, the vibrating mesh nebulizer has become popular owing to its compactness and noiselessness. In this study, an experimental system is proposed to measure the deposition fraction (DF) of nebulized sodium chloride (NaCl) droplets in an idealized mouth-throat airway model. The results show that before the DF increases to 58.6% with an increasing flow rate to 60 L/min, there is a decrease in DF from 42.4% to 15.5% when the inhalation flow rate increases from 15 to 22.5 L/min for a normal saline solution. These results substantially differ from the conclusions of dry powder or particle experiments and simulations, which monotonously increases with increasing inhalation flow rate. This suggests that droplet evaporation during aerosol generation and transport in the airway plays an important role. The experiment also showed that droplets generated from solutions with a higher NaCl concentration have higher DFs.

Keywords: vibrating mesh nebulizer; deposition fraction; droplet; airway model; temperature and humidity



Citation: Xia, X.; Ding, T.; Chen, X.; Tao, F.; Sun, B.; Lu, T.; Wang, J.; Huang, Y.; Xu, Y. Evaporation Affects the In Vitro Deposition of Nebulized Droplet in an Idealized Mouth-Throat Model. *Atmosphere* **2023**, *14*, 93. https://doi.org/10.3390/ atmos14010093

Academic Editors: Kai-Jen Chuang and Daniele Contini

Received: 2 December 2022 Revised: 27 December 2022 Accepted: 29 December 2022 Published: 31 December 2022



Copyright: © 2022 by the authors. Licensee MDPI, Basel, Switzerland. This article is an open access article distributed under the terms and conditions of the Creative Commons Attribution (CC BY) license (https://creativecommons.org/licenses/by/4.0/).

1. Introduction

Respiratory diseases impose a substantial medical burden and reduce the quality of life [1–3]. Inhalation therapy, which treats respiratory diseases, has typical advantages, e.g., higher drug concentrations in pulmonary tissue, rapid onset, and fewer side effects [4]. Nebulizer is one of the most common devices for inhalation therapy [5,6]. During the pandemic of novel coronavirus disease 2019 (COVID-19), nebulizers were also widely used to generate droplet aerosol carrying the COVID-19 vaccine [7].

The human airway has a complex geometry, affecting the airflow and particle/droplet deposition. Experiments and simulations have been conducted to analyze the transport and deposition of aerosol during inhalation [8-10]. Turbulent laryngeal jet [11,12], secondary flow, and other transient airflow structures [13] lead to different aerosol deposition characteristics. Inertial impact is the leading mechanism for the deposition of micron particles in the upper respiratory tract. The micron particles' deposition fraction (DF) increases with particle density, size, velocity, etc. [14]. Grgic et al. [15] obtained the overall deposition efficiency and localized deposition pattern by extracting the position and intensity of radioactive particles in an idealized human mouth-throat (MT) model. Considering the realistic geometric features of the respiratory tract, Golshahi et al. [16] proposed correlations for predicting the deposition of micron particles in the oropharyngeal airway of children aged 6-14 years at medium-to-high inhalation flow rates. Xi et al. [17] successfully measured the droplet deposition patterns in upper airway models using Sar gel. Zhang et al. [18] concluded that oral airway constriction at moderate-to-high flow rates increases particle deposition in the laryngeal airways. Feng et al. [19] recently provided a tutorial for the simulations of transport, deposition, and translocation of particles in human airways.

Atmosphere 2023, 14, 93 2 of 10

Compared to traditional nebulizers, i.e., jet nebulizers and ultrasonic nebulizers, the vibrating mesh nebulizer (VMN) has become popular owing to its portability and noiselessness, among other advantages. Waldrep and Dhand. [20] introduced unique design features of different VMNs, including MicroAir, Aeroneb, eFlow, and I-neb. Galindo-Filho et al. [21] used radiolabeled aerosols to evaluate the in vivo pulmonary DF of droplets generated by VMNs and jet nebulizers during noninvasive ventilation. They showed that VMNs delivered two-fold more aerosols into the respiratory tract compared with jet nebulizers. Pulmonary aerosol deposition from SPECT-CT analysis increased by six times with the Aerogen Ultra VMN compared to the Opti-Mist Plus jet nebulizer [22]. In vivo experiments also showed that the eFlow rapid VMN was more efficient in terms of lung deposition and drug output for amikacin nebulization than the Sidestream jet nebulizer [23].

The nebulized droplets contain a normal saline solution and dissolved drug components or nondissolvable small drug particles. Thus, evaporation of multicomponent droplet is one of the key factors, which could change the droplet trajectory and affect the deposition in the airway. For multicomponent droplets, experimental results show that the solute-induced water vapor–pressure reduction considerably slows the evaporation process and dominates the solute-concentration dependence of droplet evaporation time [24]. Sasaki et al. [25] found that the evaporation of ethanol and water binary droplets had three stages: (1) preferential evaporation of ethanol, (2) transition (evaporation of ethanol and condensation of water), and (3) evaporation and condensation of water. Zeng et al. [26] showed that humidity distribution significantly affects evaporation of droplets with solid fractions when simulating the transport of exhaled aerosols into ambient air. Dbouk and Drikakis. [27] suggested that the influence of the environment's relative humidity and temperature on droplet evaporation needs to be quantified for the transmission of exhaled droplets. A high-speed camera is often used to capture the evolution of large droplets [28,29], which could be used to validate the mathematic models.

It is critical to capture the droplet-vapor interaction phenomenon, i.e., evaporation and condensation, to simulate a dynamic change, transport, and deposition of droplets in the human airway. Finlay [30] introduced a mathematical model describing the change in particle size due to evaporation or condensation. Zhang et al. [31] validated their droplet-vapor interaction model and studied the evaporative and hygroscopic effects and deposition of isotonic and hypertonic saline droplets in a mouth-to-G4 airway model. Furthermore, Zhang et al. [32] included the effects of humid airway boundary and 3D RH distribution of the airway in the simulations. They concluded that droplet evaporation and hygroscopic growth are important under different environmental relative humidity (RH) and temperature conditions. Chen et al. [33] achieved a higher accuracy of the droplet-vapor interaction model than Zhang et al. [32] compared with the experimental data [34]. Simulations showed that the effects of environmental RH and humid airway boundary on the deposition of droplets are important. Later on, Chen et al. [35] constructed a mucus-tissue model around the airway conduit based on a two-layer method [36] and analyzed the effects of mucus evaporation and mucus-tissue heat transfer on droplet deposition in an idealized airway. These two models were used, validated, and applied to individual airways [37,38]. Winkler-Heil et al. [39] studied the accuracy of their aerosol dynamics model when predicting the hygroscopic growth of NaCl particles and simulated the dynamic change, transport, and deposition of NaCl particles in the human airway. Wickert and Prokop. Ref. [40] reviewed the methods for simulating water evaporation under natural conditions.

VMN can generate droplets with a high number concentration. When the droplets evaporate, the RH of inhaled air will increase in the upper airway, which would in turn weaken the evaporation of droplets. The role of droplet evaporation in the upper airway deposition mechanism is still unclear for VMN. Khamooshi et al. [41] simulated the deposition of nebulized droplets in a nasal airway without considering evaporation. However,

Atmosphere 2023, 14, 93 3 of 10

overlooking the droplet evaporation would overestimate the DF up to 80% in a simplified MT airway model when using the one-way coupling method [35].

This study aimed to investigate the transport and deposition of VMN-generated droplets in a simplified MT airway [42]. An experimental system was developed to measure the droplet DF in the airway. The DFs of droplets with high concentrations were acquired under different steady inhalation flow rates. The effect of solution concentration on DF was also evaluated by comparing the DFs of droplets nebulized from 0.9% and 10% w/v NaCl solutions. Our results provide new insights into nebulized droplet deposition that can be used to model and validate droplet–vapor interaction for applications with a high droplet concentration, e.g., nebulizers, MDIs (Metered-dose Inhalers), and e-cigarettes.

2. Methods

2.1. Experimental Environment and Setup

The environment for the experiment was controlled. The experiments were conducted in a cleanroom installed in the laboratory. The temperature and RH of the cleanroom were maintained at 26.5 ± 1 °C and 50 ± 2 %, respectively. The air in the laboratory was first purified. The mass concentration of PM_{2.5} in the laboratory was 0 μ g/m³, which was monitored using a TSI DustTrak aerosol monitor 8532 (TSI Inc., Shoreview, MN, USA). The particle concentration in the ISO 4 cleanroom was verified using a TSI optical particle size spectrometer 3330 (TSI Inc., Shoreview, MN, USA).

Figure 1 shows the experimental setup of droplet deposition experiment under steady inhalation conditions. The experimental system consists of a VMN, an idealized MT model, a bubble absorption tube, a prefilter, a membrane filter, a glass rotor flowmeter, and a vacuum pump.

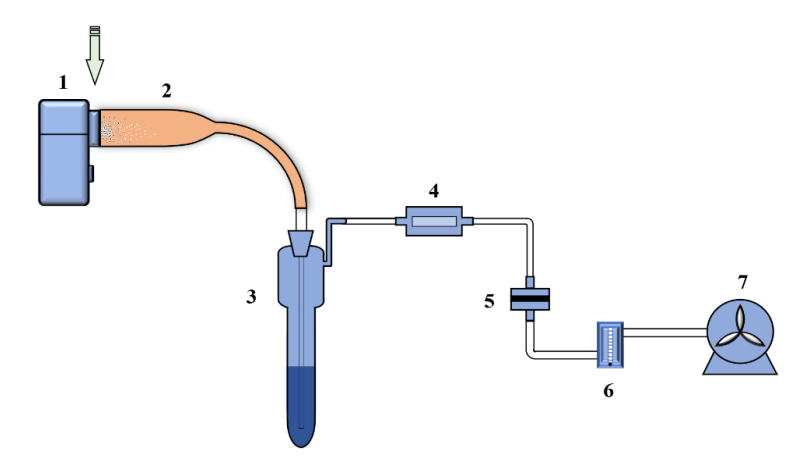


Figure 1. Schematic of experimental setup: (1) VMN, (2) idealized mouth-throat airway model, (3) bubble absorption tube, (4) prefilter, (5) membrane filter, (6) glass rotor flowmeter, (7) vacuum pump.

2.2. Vibrating Mesh Nebulizer (VMN)

A commercial VMN, HL100A (Yuwell Co., Ltd., Zhenjiang, Jiangsu, China), was used in this study (Figure 2). A piezoelectric transducer was vertically installed on the side of the reservoir, and therefore the aerosol stream is generated horizontally. There is a short tube at the outlet of the aerosol stream. It connects the silicone mouthpiece. The upper half of the short tube has a semicircular opening, which is used as the air inlet for inhalation. The nebulized droplet distributions were measured using the light scattering method (Spraylink, Zhuhai Linkoptic Instrument Co., Ltd., Zhuhai, Guangdong, China). Table 1 shows the droplet size distributions of the nebulized 0.9% and 10% $\mbox{\it w/v}$ NaCl solutions and the setting of refractive indexes. The droplet size distribution was measured in triplicate. Each measurement result is the average value of 10 times of sampling in 30 s. The nebulization rate of the liquid is 0.22 \pm 0.02 g/min, which was also measured in triplicate.

Atmosphere 2023, 14, 93 4 of 10





Figure 2. HL100A vibrating mesh nebulizer: (a) front view without mouthpiece, (b) side view with mouthpiece.

Table 1. Droplet size distributions of nebulized 0.9% and 10% w/v NaCl solutions.

Parameter	0.9% NaCl Solution	10% NaCl Solution
Refractive index	1.335	1.351
MMAD	5.82 μm	5.91 μm
Geometric standard deviation	1.447	1.602

2.3. Idealized MT Airway Model

An idealized MT model was proposed by Zhang et al. [43]. The model has a 30 mm diameter inlet and an 8.5 mm diameter outlet. Zhang et al. [43] suggested that the idealized MT airway model can mimic in vivo MT deposition of the inhalable particle. To rinse the MT airway model, the cavity of the model was divided into two symmetric halves. The aluminum MT airway model used in our experiment (Figure 3) was manufactured by computer numerical control machining and anodized to enhance the surface smoothness.

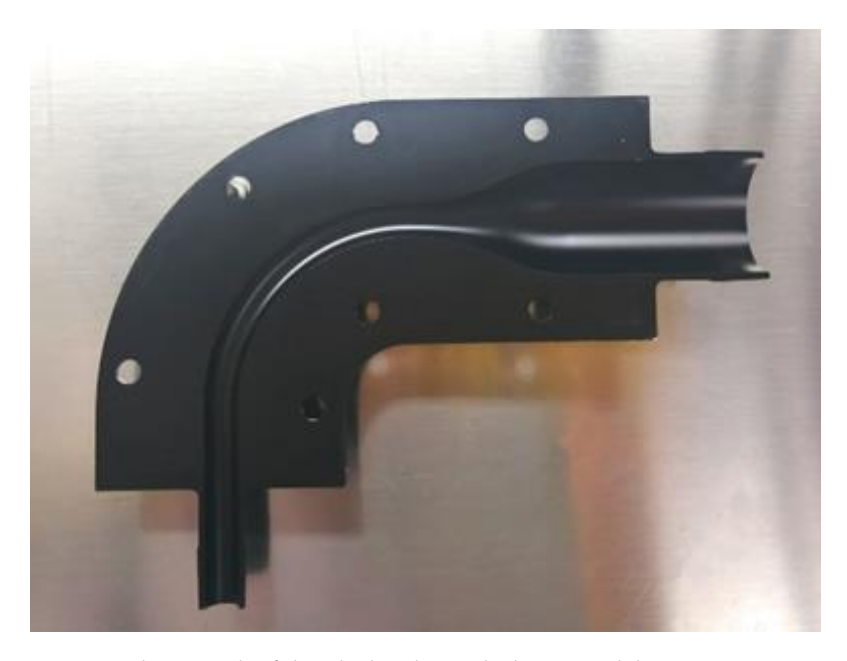


Figure 3. Photograph of the idealized mouth-throat model.

Atmosphere 2023, 14, 93 5 of 10

2.4. In Vitro Nebulization Test

For each test, the mouth cavity of the MT airway model and prefilter was installed horizontally. The bubble absorption tube, filter unit, and flowmeter were installed vertically. A glass rotor flowmeter (10–100 L/min, $\pm 4\%$, LZM-6T, Senlod Co., Ltd., Nanjing, China) was used to adjust the flow rate in the system using a vacuum pump. The VMN was activated to nebulize the NaCl solution when the flow rate was stable. The nebulization lasted 3 min to ensure the following: (1) No large droplet formed and dripped from the throat outlet into the bubble absorption tube, and (2) no large droplet formed on the membrane filter. The deionized water (Nandye Co., Ltd., Wenzhou, Zhejiang, China) in the bubble absorption tube was used to capture most droplets exiting from the MT airway model. A stainless-steel prefilter (Jingwei Co., Ltd., Shanghai, China) with a pore size of 0.5 mm was used to block the possible large droplets from bubble breakage in the bubble absorption tube. A glass fiber membrane filter (Yaxin Co., Ltd., Shanghai, China) with a pore size of 0.1 μ m collected the rest of the droplets.

After the droplet deposition, the mouthpiece of VMN, the MT airway model, bubble absorption tube, prefilter, a membrane filter, and the tubes used to connect these parts were detached from the system. Using deionized water, these components were rinsed in ultrasonic cleaners (Huace Science and Technology Co., Ltd., Shenzhen, Guangdong, China). The rinsate was collected in volumetric flasks, and the volume was adjusted with deionized water.

The samples were assayed to quantify the NaCl deposition in the mouthpiece, MT airway model, bubble absorption tube, prefilter, a membrane filter, and tubes using an automatic potentiometric titrator (PXSJ-216F, INESA Scientific Instrument Co., Ltd., Shanghai, China). The potentiometric titrator measured the volume concentration of the chloride ion. Therefore, the mass of NaCl in the sample could be calculated based on the Cl⁻ concentration and the volume of volumetric flask. The difference between the NaCl mass in the nebulized solution and the NaCl mass in the rinsate was less than 5% for each test, ensuring that almost all nebulized droplets were captured.

The experiments were conducted under five inhalation flow rates of 15, 22.5, 30, 45, and 60 L/min and two sodium chloride (NaCl) solution concentrations of 0.9% and 10% w/v. The experiments under each condition were carried out in triplicate.

2.5. DF

The DF can be defined as follows:

$$DF = \frac{m_1}{m_1 + m_2} \times 100\% \tag{1}$$

where m_1 is the mass of NaCl droplets deposited in the mouthpiece and MT model and m_2 is the mass of NaCl droplets escaped from the MT model. m_2 includes the mass of NaCl droplets captured by the bubble absorption tube, prefilter, membrane filter, and tubes connecting these components. A high DF in the MT airway indicates that fewer droplets could be delivered into the lung.

3. Results and Discussion

Figure 4 shows the DFs in the MT airway model as a function of the inertial parameter, $\rho_{\rm d}d_{\rm d}^2Q$, where the $\rho_{\rm d}$ (g/cm³) is the droplet density, $d_{\rm d}$ (µm) is the MMAD of the droplet, and Q (cm³/s) is the inhalation flow rate. The black squares and red dots in Figure 4 show the DFs of the droplets of nebulized 0.9% and 10% w/v NaCl solution in the MT model, respectively. The blue triangles are the experimental results of the DEHS (Di-Ethyl-Hexyl-Sebacat) oil droplets in the same MT model [43].

Atmosphere 2023, 14, 93 6 of 10

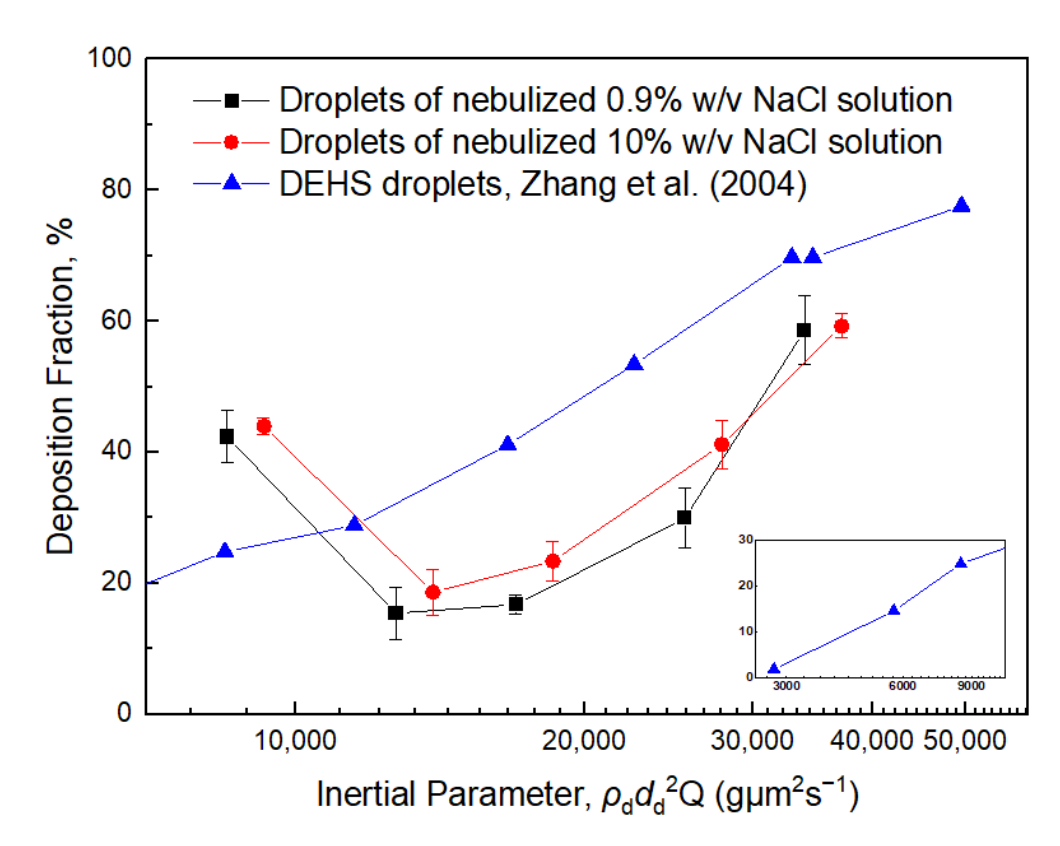


Figure 4. DF of different droplets in the idealized mouth-throat airway as a function of inertial parameter.

3.1. Effect of Inhalation Flow Rate

Normal saline, a solution of 0.9%~w/v NaCl, is the most common medium to dissolve or disperse drugs for inhalation therapy when using nebulizers. Therefore, the DFs of droplets of nebulized normal saline (the black dots in Figure 4) in the MT model were tested. When the inhalation flow rate increased, the DF of droplets decreased from 42.4% at $15~\rm L/min$ to 15.5% at $22.5~\rm L/min$ and then the DF gradually increased to 16.8% at $30~\rm L/min$. The DF increased continuously with the increase in the inhalation flow rate to 29.9% and 58.6% at $45~\rm and$ $60~\rm L/min$, respectively.

The variation in the DFs of normal saline droplets as a function of inertial parameter is different from the previous experiment. Zhang et al. [43] used DEHS droplets, which did not evaporate or condense in the air, to evaluate the deposition characteristics of MT model. The DF of DEHS droplets only increased monotonically with the increase in inertial parameter. However, similar decreases and then increases in the DFs or deposition efficiencies of the particles or droplets were previously reported. Kleinstreuer et al. [44] reported the main mechanism for the particle DF in the human upper airway as a function of particle diameter. It was concluded that the DFs decrease for ultrafine particles (0.01 to 1 µm) because of a reduction in diffusive capacity, while the DFs increased for micron particles due to increasing impaction when the particle diameter increased from 1 µm to 10 µm. Chen et al. [45] found that the minimum deposition efficiency exists for micron particles in a G11-G14 lung airway. The numerical predictions show that the deposition efficiencies of 5 and 7 µm particles first decreased with the increase in inhalation flow rate and then increased with the inhalation flow rate again. These results indicate that the main deposition mechanism changes between sedimentation and impaction. It is well known that the DFs of droplets or particles increase with the increase in the inhalation flow rate in the airway. Therefore, there must be a mechanism that leads to a decrease in the DF of nebulized normal saline droplets in this study when the inhalation flow rate increased from 15 to 22.5 L/min.

Atmosphere 2023, 14, 93 7 of 10

A possible explanation is that the droplet size changes due to evaporation. However, simply considering the droplet residence time cannot explain this phenomenon. For example, droplets would have the longest residence time at 15 L/min; therefore, they would have the longest time to evaporate in the airway model. The droplets also have the lowest inertia due to the lowest air velocity in this experiment. Then, the DF of droplets should be the lowest under 15 L/min condition, which is different from our result. Thus, the mass balance of water between the droplets and air needs to be considered.

If the water in the normal saline droplets generated by the VMN entirely evaporated, the RH of well-mixed air would approximately reach 103%, 85%, 76%, 67%, and 63% at inhalation flow rates of 15, 22.5, 30, 45, and 60 L/min, respectively. Experiments indicated an RH threshold for NaCl to absorb water vapor or precipitation from an aqueous solution. Tang et al. [46] suggested that the deliquescence point for the NaCl aerosol is approximately an RH of 76% at 25 $^{\circ}$ C. Robinson and Stokes [47] found that the deliquescence point is an RH of 75.3% for a bulk NaCl solution. Cruz and Pandis [48] reported that a 100 nm NaCl particle could grow under an RH of 75% at 22 $^{\circ}$ C to 26 $^{\circ}$ C. Thus, the saline droplets would partially evaporate but arrive at different equilibrium statuses under 15 and 22.5 L/min flow rates. The droplets would evaporate more efficiently and become solid NaCl particles under inhalation flow rates of 45 and 60 L/min conditions.

We can deduce that the droplet evaporation and inertial impact are the two main mechanisms governing the deposition, first decreasing and then increasing the DFs as a function of inertial parameter, as shown in Figure 4. This is an analogy to the change in deposition mechanism from inertial impact to Brownian motion when the particle size decreases from micrometers to nanometers in the upper airway [44] or the change in deposition mechanism between the inertial impact and gravitational sedimentation in the lower airway [45]. The evaporation of droplets reduces the possibility of inertial impaction and sedimentation; therefore, the droplets have lower DFs at flow rates of 22.5 and 30 L/min. When most droplets evaporate, the DF increases with the flow rate due to increased droplet/particle inertia at 45 and 60 L/min.

3.2. Effect of NaCl Solution Concentration

The red circles shown in Figure 4 are the DFs of $10\% \ w/v$ NaCl droplets. When the inhalation flow rate increases, the DF of droplets first decreased from 43.9% at 15 L/min to 18.6% at 22.5 L/min and then the DF gradually increased to 23.4% at 30 L/min. The DF continuously increased with the increase in the inhalation flow rate to 41.2% and 59.3% at 45 and 60 L/min, respectively.

Considering that the mass median aerodynamic diameter (MMAD) of droplets of 10% w/v NaCl solution is slightly larger than that of 0.9% w/v NaCl solution; the inertial parameters of 10% w/v NaCl droplets are more significant than those of 0.9% w/v NaCl droplets (black squares shown in Figure 4) at the same inhalation flow rate conditions. The DFs of 10% w/v NaCl droplets are higher than those of 0.9% w/v NaCl droplets in the range of inertial parameters from 9000 to 37,000 gµm²/s in general, as shown in Figure 4.

We assume that the droplets could not be entirely evaporated at inhalation flow rates of 15 and 22.5 L/min. The molar fraction of water is lower in the droplet if the droplet initially has a higher NaCl concentration. Thus, the water molecule is less likely to escape the droplet surface and enter the air at the same environmental RH. This reduces the evaporation rate of droplet with a higher NaCl concentration. The droplet with a higher NaCl concentration, which has a lower evaporation rate, is relatively larger than that with a lower NaCl concentration for the same initial diameter when evolving with time. Thus, the droplet with a higher NaCl concentration has a higher possibility of settling in the airway if the inhalation flow rate is low. It also has a higher inertia than that with a lower NaCl concentration when flowing through the MT airway. The increased inertia leads to a higher possibility of depositing on the airway surface due to inertial impact.

For higher inhalation flow rates, i.e., 30 to 60 L/min, we can assume that the droplets could evaporate more efficiently. The droplet with a higher NaCl concentration would

Atmosphere 2023, 14, 93 8 of 10

have a larger dry NaCl particle size when fully evaporated for the same initial droplet size. Therefore, a larger particle leads to a higher DF.

According to the results of our experiment, decreasing the nebulizing rate of this commercial VMN could increase the delivery efficiency of the droplet in the patient's lung. Note that the nebulizer inhalation therapy often operates at a low inhalation flow rate, e.g., lower than 20 L/min [49]. This is approximately the value of inertial parameter of 10,000 shown in Figure 4. Under this condition, increasing the inhalation flow rate or diluting the droplet flow can reduce the DF in the MT airway. Decreasing the nebulizing rate of HL100A VMN can reduce the mass of droplets per unit volume of inhaled air; therefore, it can reduce the DF of droplets in the upper airway.

4. Conclusions

The deposition experiments of droplets generated from a commercial VMN were conducted in an idealized MT airway model. An in vitro experiment system was established to measure the DF of droplets in the airway model. Solutions with two NaCl concentrations, i.e., 0.9% and $10\% \ w/v$, were nebulized at different inhalation flow rates from 15 to 60 L/min. A relationship between the DFs of nebulized droplets and inertial parameters at different inhalation flow rates was obtained. Based on the results from our experimental study, we conclude the following:

- 1. The DF of nebulized droplets first decreases with the increase in inhalation flow rate and then increases with the inhalation flow rate again. This deposition characteristic significantly differs from the experiments for solid particles or DEHS droplets;
- The high DF of VMN nebulized droplets at 15 L/min is caused by the humidification
 of inhaled air due to droplet evaporation. The increase in air RH handicaps the
 droplet evaporation, if the RH is higher than the threshold for the hygroscopic growth
 of NaCl;
- Droplets nebulized from a solution with a higher NaCl concentration have a higher DF in the MT airway.

Limitations and Future Work

Our experimental study provides a macroscopic measurement of the DF of nebulized droplets in an upper airway model. Distinct differences have been observed compared to the results of deposition experiments of dry particles. This study has established the experiment system and procedures to evaluate the DF of droplet aerosol in the airway model. Future work may focus on the characteristics of VMN and environmental conditions affecting the droplet transport and deposition, i.e.,

- 1. Nebulization rate of VMN, which may change the water vapor transfer between the droplets and surrounding air;
- 2. Structure of VMN air inlet, which may change the trajectory of droplet;
- A realistic inhalation waveform instead of a steady inhalation flow rate, which may change the DF and deposition pattern of the droplets;
- 4. Environmental temperature and humidity may also change the water vapor transfer between the droplets and air.

Author Contributions: Conceptualization, X.X., T.D. and X.C.; methodology, X.X., T.D., X.C., F.T. and B.S.; software, J.W. and Y.H.; validation, T.D. and Y.X.; formal analysis, X.X., T.D. and F.T.; investigation, X.X., T.D., F.T. and B.S.; resources, T.L. and Y.X.; data curation, T.D., F.T. and T.L.; writing—original draft preparation, X.X., T.D. and X.C.; writing—review and editing, X.X., X.C., F.T., J.W. and Y.X.; visualization, T.D., J.W. and Y.H.; supervision, X.C. and T.L.; project administration, X.X., X.C. and Y.X.; funding acquisition, X.C. and B.S. All authors have read and agreed to the published version of the manuscript.

Funding: The authors gratefully acknowledge the financial support of the National Natural Science Foundation of China (Grant No. 51976091), Qinglan Project of Jiangsu Province, and Postgraduate Research & Practice Innovation Program of Jiangsu Province, China (KYCX22_1618).

Atmosphere 2023, 14, 93 9 of 10

Institutional Review Board Statement: Not applicable.

Informed Consent Statement: Not applicable.

Data Availability Statement: The data that support the findings of this study are available from the corresponding author upon reasonable request.

Conflicts of Interest: The authors declare no conflict of interest.

References

1. Arpinelli, F.; Carone, M.; Riccardo, G.; Bertolotti, G. Health-related quality of life measurement in asthma and chronic obstructive pulmonary disease: Review of the 2009–2014 literature. *Multidiscip. Respir. Med.* **2016**, *11*, 1–7. [CrossRef]

- 2. WHO. 10 Facts on Asthma. Available online: https://www.who.int/features/factfiles/asthma/en/ (accessed on 4 January 2022).
- WHO. Chronic Respiratory Diseases-Burden of COPD. Available online: https://www.who.int/respiratory/copd/burden/en/ (accessed on 4 January 2022).
- 4. Ehrmann, S. Vibrating mesh nebulisers—can greater drug delivery to the airways and lungs improve respiratory outcomes. *Eur. Respir. Pulmon. Dis.* **2018**, *4*, 33–43. [CrossRef]
- 5. Dhand, R.; Dolovich, M.; Chipps, B.R.; Myers, T.; Restrepo, R.; Rosen Farrar, J. The role of nebulized therapy in the management of COPD: Evidence and recommendations. *COPD J. Chronic Obstr. Pulm. Dis.* **2012**, *9*, 58–72. [CrossRef] [PubMed]
- 6. Di Cristo, L.; Maguire, C.M.; Mc Quillan, K.; Aleardi, M.; Volkov, Y.; Movia, D.; Prina-Mello, A. Towards the identification of an in vitro tool for assessing the biological behavior of aerosol supplied nanomaterials. *Int. J. Environ. Res. Public Health* **2018**, 15, 563. [CrossRef]
- 7. Wu, S.; Huang, J.; Zhang, Z.; Wu, J.; Zhang, J.; Hu, H.; Zhu, T.; Zhang, J.; Luo, L.; Fan, P. Safety, tolerability, and immunogenicity of an aerosolised adenovirus type-5 vector-based COVID-19 vaccine (Ad5-nCoV) in adults: Preliminary report of an open-label and randomised phase 1 clinical trial. *Lancet Infect. Dis.* **2021**, 21, 1654–1664. [CrossRef] [PubMed]
- 8. Islam, M.S.; Paul, G.; Ong, H.X.; Young, P.M.; Gu, Y.T.; Saha, S.C. A review of respiratory anatomical development, air flow characterization and particle deposition. *Int. J. Environ. Res. Public Health* **2020**, *17*, 380. [CrossRef]
- 9. Singh, P.; Raghav, V.; Padhmashali, V.; Paul, G.; Islam, M.S.; Saha, S.C. Airflow and particle transport prediction through stenosis airways. *Int. J. Environ. Res. Public Health* **2020**, *17*, 1119. [CrossRef]
- 10. Islam, M.S.; Larpruenrudee, P.; Hossain, S.I.; Rahimi-Gorji, M.; Gu, Y.; Saha, S.C.; Paul, G. Polydisperse aerosol transport and deposition in upper airways of age-specific lung. *Int. J. Environ. Res. Public Health* **2021**, *18*, 6239. [CrossRef]
- 11. Choi, J.; Tawhai, M.H.; Hoffman, E.A.; Lin, C.-L. On intra-and intersubject variabilities of airflow in the human lungs. *Phys. Fluids* **2009**, *21*, 101901. [CrossRef] [PubMed]
- 12. Fan, Y.; Dong, J.; Tian, L.; Inthavong, K.; Tu, J. Numerical and experimental analysis of inhalation airflow dynamics in a human pharyngeal airway. *Int. J. Environ. Res. Public Health* **2020**, *17*, 1556. [CrossRef]
- 13. Zhang, Z.; Kleinstreuer, C. Transient airflow structures and particle transport in a sequentially branching lung airway model. *Phys. Fluids* **2002**, *14*, 862–880. [CrossRef]
- 14. Kleinstreuer, C.; Zhang, Z. Airflow and particle transport in the human respiratory system. *Annu. Rev. Fluid Mech.* **2010**, 42, 301–334. [CrossRef]
- 15. Grgic, B.; Finlay, W.; Heenan, A. Regional aerosol deposition and flow measurements in an idealized mouth and throat. *J. Aerosol Sci.* **2004**, *35*, 21–32. [CrossRef]
- 16. Golshahi, L.; Noga, M.L.; Finlay, W.H. Deposition of inhaled micrometer-sized particles in oropharyngeal airway replicas of children at constant flow rates. *J. Aerosol Sci.* **2012**, *49*, 21–31. [CrossRef]
- 17. Xi, J.; Wang, Z.; Si, X.A.; Zhou, Y. Nasal dilation effects on olfactory deposition in unilateral and bi-directional deliveries: In vitro tests and numerical modeling. *Eur. J. Pharm. Sci.* **2018**, *118*, 113–123. [CrossRef] [PubMed]
- 18. Zhang, Z.; Kleinstreuer, C.; Kim, C. Micro-particle transport and deposition in a human oral airway model. *J. Aerosol Sci.* **2002**, *33*, 1635–1652. [CrossRef]
- 19. Feng, Y.; Zhao, J.; Hayati, H.; Sperry, T.; Yi, H. Tutorial: Understanding the transport, deposition, and translocation of particles in human respiratory systems using Computational Fluid-Particle Dynamics and Physiologically Based Toxicokinetic models. *J. Aerosol Sci.* **2021**, *151*, 105672. [CrossRef]
- 20. Waldrep, J.; Dhand, R. Advanced nebulizer designs employing vibrating mesh/aperture plate technologies for aerosol generation. *Curr. Drug Deliv.* **2008**, *5*, 114–119. [CrossRef]
- 21. Galindo-Filho, V.C.; Ramos, M.E.; Rattes, C.S.; Barbosa, A.K.; Brandão, D.C.; Brandão, S.C.S.; Fink, J.B.; de Andrade, A.D. Radioaerosol pulmonary deposition using mesh and jet nebulizers during noninvasive ventilation in healthy subjects. *Respir. Care.* 2015, 60, 1238–1246. [CrossRef]
- 22. Dugernier, J.; Hesse, M.; Vanbever, R.; Depoortere, V.; Roeseler, J.; Michotte, J.-B.; Laterre, P.-F.; Jamar, F.; Reychler, G. SPECT-CT comparison of lung deposition using a system combining a vibrating-mesh nebulizer with a valved holding chamber and a conventional jet nebulizer: A randomized cross-over study. *Pharm. Res.* 2017, 34, 290–300. [CrossRef]
- 23. Pitance, L.; Vecellio, L.; Leal, T.; Reychler, G.; Reychler, H.; Liistro, G. Delivery efficacy of a vibrating mesh nebulizer and a jet nebulizer under different configurations. *J. Aerosol Med. Pulm. Deliv.* **2010**, 23, 389–396. [CrossRef]

Atmosphere 2023, 14, 93 10 of 10

24. Rezaei, M.; Netz, R.R. Water evaporation from solute-containing aerosol droplets: Effects of internal concentration and diffusivity profiles and onset of crust formation. *Phys. Fluids* **2021**, *33*, 091901. [CrossRef]

- 25. Sasaki, Y.; Hasegawa, K.; Kaneko, A.; Abe, Y. Heat and mass transfer characteristics of binary droplets in acoustic levitation. *Phys. Fluids* **2020**, *32*, 072102. [CrossRef]
- 26. Zeng, G.; Chen, L.; Yuan, H.; Yamamoto, A.; Maruyama, S. Evaporation flow characteristics of airborne sputum droplets with solid fraction: Effects of humidity field evolutions. *Phys. Fluids* **2021**, *33*, 123308. [CrossRef]
- Dbouk, T.; Drikakis, D. On coughing and airborne droplet transmission to humans. Phys. Fluids 2020, 32, 053310. [CrossRef]
 [PubMed]
- 28. Ju, W.; Wu, Y.; Lin, S.; Zhao, F.; Tan, S. Visual experimental study of droplet impinging on liquid film and analysis of droplet evolution characteristics. *Exp. Comput. Multiph. Flow* **2020**, *4*, 212–220. [CrossRef]
- 29. Wang, Q.; Wang, Z.; Jiang, Y.; Yang, S. Experimental study of electro-spraying modes of deionized water in atmospheric environment. *Exp. Comput. Multiph. Flow* **2019**, *3*, 38–46. [CrossRef]
- 30. Finlay, W.H. The Mechanics of Inhaled Pharmaceutical Aerosols: An Introduction; Academic Press: New York, NY, USA, 2001.
- 31. Zhang, Z.; Kleinstreuer, C.; Kim, C.S. Isotonic and hypertonic saline droplet deposition in a human upper airway model. *J. Aerosol Med.* 2006, 19, 184–198. [CrossRef]
- 32. Zhang, Z.; Kim, C.S.; Kleinstreuer, C. Water vapor transport and its effects on the deposition of hygroscopic droplets in a human upper airway model. *Aerosol Sci. Technol.* **2006**, 40, 1–16. [CrossRef]
- 33. Chen, X.; Feng, Y.; Zhong, W.; Kleinstreuer, C. Numerical investigation of the interaction, transport and deposition of multicomponent droplets in a simple mouth-throat model. *J. Aerosol Sci.* **2017**, *105*, 108–127. [CrossRef]
- 34. Tu, H.; Ray, A.K. Measurement of activity coefficients from unsteady state evaporation and growth of microdroplets. *Chem. Eng. Commun.* **2005**, 192, 474–498. [CrossRef]
- 35. Chen, X.; Kleinstreuer, C.; Zhong, W.; Feng, Y.; Zhou, X. Effects of thermal airflow and mucus-layer interaction on hygroscopic droplet deposition in a simple mouth–throat model. *Aerosol Sci. Technol.* **2018**, 52, 900–912. [CrossRef]
- 36. Wu, D.; Tawhai, M.H.; Hoffman, E.A.; Lin, C.-L. A numerical study of heat and water vapor transfer in MDCT-based human airway models. *Ann. Biomed. Eng.* **2014**, *42*, 2117–2131. [CrossRef]
- Rajaraman, P.K.; Choi, J.; Hoffman, E.A.; O'Shaughnessy, P.T.; Choi, S.; Delvadia, R.; Babiskin, A.; Walenga, R.; Lin, C.-L. Transport and deposition of hygroscopic particles in asthmatic subjects with and without airway narrowing. *J. Aerosol Sci.* **2020**, *146*, 105581. [CrossRef]
- 38. Xu, C.; Zheng, X.; Shen, S. A numerical study of the effects of ambient temperature and humidity on the particle growth and deposition in the human airway. *Environ. Res.* **2021**, 200, 111751. [CrossRef]
- 39. Winkler-Heil, R.; Pichelstorfer, L.; Hofmann, W. Aerosol dynamics model for the simulation of hygroscopic growth and deposition of inhaled NaCl particles in the human respiratory tract. *J. Aerosol Sci.* **2017**, *113*, 212–226. [CrossRef]
- 40. Wickert, D.; Prokop, G. Simulation of water evaporation under natural conditions—A state-of-the-art overview. *Exp. Comput. Multiph. Flow.* **2021**, 3, 242–249. [CrossRef]
- 41. Khamooshi, M.; Fletcher, D.F.; Salati, H.; Vahaji, S.; Gregory, S.; Inthavong, K. Computational assessment of the nasal air conditioning and paranasal sinus ventilation from nasal assisted breathing therapy. *Phys. Fluids* **2022**, *34*, 051912. [CrossRef]
- 42. Zhang, Y.; Finlay, W.; Matida, E. Particle deposition measurements and numerical simulation in a highly idealized mouth–throat. *J. Aerosol Sci.* **2004**, *35*, 789–803. [CrossRef]
- 43. Zhang, Y.; Chia, T.L.; Finlay, W.H. Experimental measurement and numerical study of particle deposition in highly idealized mouth-throat models. *Aerosol Sci. Technol.* **2006**, *40*, 361–372. [CrossRef]
- 44. Kleinstreuer, C.; Zhang, Z.; Li, Z. Modeling airflow and particle transport/deposition in pulmonary airways. *Resp. Physiol. Neurobiol.* **2008**, *163*, 128–138. [CrossRef] [PubMed]
- 45. Chen, X.; Feng, Y.; Zhong, W.; Sun, B.; Tao, F. Numerical investigation of particle deposition in a triple bifurcation airway due to gravitational sedimentation and inertial impaction. *Powder Technol.* **2018**, 323, 284–293. [CrossRef]
- 46. Tang, I.; Munkelwitz, H.; Davis, J. Aerosol growth studies—II. Preparation and growth measurements of monodisperse salt aerosols. *J. Aerosol Sci.* 1977, 8, 149–159. [CrossRef]
- 47. Robinson, R.A.; Stokes, R.H. Electrolyte Solutions; Butterworth: London, UK, 1970.
- 48. Cruz, C.N.; Pandis, S.N. Deliquescence and hygroscopic growth of mixed inorganic-organic atmospheric aerosol. *Environ. Sci. Technol.* **2000**, *34*, 4313–4319. [CrossRef]
- 49. Zhou, Y.; Brasel, T.L.; Kracko, D.; Cheng, Y.-S.; Ahuja, A.; Norenberg, J.P.; William Kelly, H. Influence of impactor operating flow rate on particle size distribution of four jet nebulizers. *Pharm. Dev. Technol.* **2007**, *12*, 353–359. [CrossRef] [PubMed]

Disclaimer/Publisher's Note: The statements, opinions and data contained in all publications are solely those of the individual author(s) and contributor(s) and not of MDPI and/or the editor(s). MDPI and/or the editor(s) disclaim responsibility for any injury to people or property resulting from any ideas, methods, instructions or products referred to in the content.